Received: 9 June 2019 | Revised: 9 June 2019 | Accepted: 11 June 2019

DOI: 10.1111/ijac.13317

International Journal of Applied Ceramic Technology

SPECIAL ISSUE ARTICLE

Dissolution, bioactivity behavior, and cytotoxicity of rare earth-containing bioactive glasses (RE = Gd, Yb)

Telma Zambanini[1] | Roger Borges[1] | Pamela C. Faria[1] | Giulia P. Delpino[1] | Isis S. Pereira[1] | Márcia M. Marques[2] | Juliana Marchi[1]

[1]Centro de Ciências Naturais e Humanas, Universidade Federal do ABC, Santo André, Brasil

[2]Departamento de Dentística, Faculdade de Odontologia, Universidade de São Paulo, São Paulo, Brasil

Correspondence
Juliana Marchi, Center for Humanities and Natural Science, Federal University of ABC, Av. dos Estados, 5001, Bangu, Santo André, SP 09210-580, Brazil.
Email: juliana.marchi@ufabc.edu.br

Funding information
Conselho Nacional de Desenvolvimento Científico e Tecnológico, Grant/Award Number: Roger Borges/130637/2016-5 and Telma Zambanini/1574811/2016; Coordenação de Aperfeiçoamento de Pessoal de Nível Superior; Fundação de Amparo à Pesquisa do Estado de São Paulo, Grant/Award Number: Giulia P. Delpino/2017/18753-6, Juliana Marchi/2011/19924-2 and Juliana Marchi/2016/16512-9

Abstract

Rare earth-containing bioactive glasses (RE-BGs) have been poorly explored in the biomaterials field, although RE has optical, nuclear, and magnetic properties that could be used in different biomedical applications. In order to verify whether these glasses can be promising as biomaterials, we studied the dissolution, bioactivity, and cytotoxicity of RE-BGs based on the SiO_2–Na_2O–CaO–P_2O_5–RE_2O_3 (RE = Gd, Yb) system. The glasses were obtained by melting-quenching and their particle size was determined by laser diffraction. Their dissolution behavior was studied in Tris-HCl, while bioactivity was performed in simulated body fluid solution under physiological conditions during several periods. The cytotoxicity test was performed using glass-derived conditioned medium and mesenchymal stem cell derived from deciduous teeth. The dissolution results showed that the glasses dissolved under two different kinetics, which are lower for rare earth-containing glasses, due to the more covalent character of Si–O–RE bonds. The bioactivity results evidenced that all glasses showed bioactivity after 24 hours. However, gadolinium and ytterbium promoted a more calcium phosphate deposition, which contrasts with the slower dissolution kinetics of rare earth-containing glasses. All the glasses were considered biocompatible, showing cell viability higher than 80%. The overall results showed that RE-BGs are promising materials for applications that require bioactivity and/or biocompatibility.

KEYWORDS
bioactive glass, bioactivity, rare earths

1 | INTRODUCTION

Rare earth (RE) are interesting elements to be used in biomedical applications because of their intrinsic properties, which make them versatile elements with a wide range of different properties. For example, concerning optical properties, the electrons of 4*f* level in RE are localized and shielded by outer 5*p* and 5*s* shells, which enable the absorption, emission, and excitation of light within the 4*f* and 5*d* orbitals, making these elements promising for luminescence applications.[1] In relation to nuclear properties, RE have radioisotopes with suitable nuclear characteristics (eg, half-life, β-decay, γ-emission, tissue penetration) to be used in brachytherapy, such as iridium-192 (^{192}Ir), iodine-125 (^{125}I), cesium-137 (^{137}Cs), palladium-103 (^{103}Pd), and cobalt-60 (^{60}Co).[2–5]

However, either in luminescence or in radiotherapy applications, rare earth needs to be host in a biocompatible matrix if biomedical applications are intended. In this sense, bioceramics become promise materials to be used as a matrix for rare earth elements. Calcium phosphate-based ceramics

(like beta-tricalcium phosphate or hydroxyapatite) and bioactive glasses are examples of bioactive ceramics successfully used in biomedical applications in the last decades.[6] Usually, these ceramics are used in bone regeneration applications, since they promote osteoconduction, angiogenesis and induce the formation of new bone tissue, but when doped with therapeutic elements, such as Ag, Sr, B, Cu, Ga, rare earth, among others, other properties can be added in these ceramics, enabling their applications beyond bone regeneration.[7,8] Nonetheless, bioactive glasses show an advantage compared with other crystalline bioceramics, due to its glass nature, it is possible to add more fractions of therapeutic elements in the glass structure without leading to the formation of secondary phases,[9] which is a limitation in crystalline materials. Therefore, bioactive glasses become favorable materials to be used together with therapeutic ions, including rare earth.

Rare earth-containing bioactive glasses, contrarily, have been poorly explored in the field of biomaterials. Most of the works in the literature reporting rare earth-containing bioactive glasses are related to applications of such glasses as seeds for brachytherapy. Indeed, the very first work reporting bioactive glasses-containing ^{153}Sm was proposed by Roberto and colleagues,[10,11] and since then other works proposed similar systems but containing holmium, rhenium, ytterbium, and yttrium.[3,4,12–16] The antioxidant potential of cerium incorporated in bioactive glasses was also reported in the literature, which is one of the most relevant studies in the field since they established a correlation between cerium oxidation in the glass structure and biological properties.[17–20]

In a previous study,[21] we comprehensively studied the structure of bioactive glasses containing gadolinium and ytterbium aiming to understand the role of rare earth in the glass structure. We reported that rare earth either act as glass formers or glass modifiers in the glass structure, although the major part is found as glass modifier. Consequently, rare earth-containing bioactive glasses tend to have a less connected glass network. In this work, we want to understand how these changes in glass structure can affect biological properties, such as dissolution, bioactivity, and cytotoxicity. Two different rare earths were chosen to evaluate their in vitro biological behavior, gadolinium or ytterbium. Gadolinium is a proper element as a contrast agent for magnetic resonance imaging due to its paramagnetic properties and relaxation time in the order of nanosecond.[22] ^{169}Yb exhibit suitable properties for brachytherapy (half-life of 32 days and mean gamma-ray energy of 93 keV)[2] and works as a sensitizing species in host matrices for luminescence applications.[1,23] Therefore, by establishing the relationship between glass structure and biological properties, this study provides a better background about rare earth-containing bioactive glasses in order to encourage further studies.

2 | MATERIALS AND METHODS

2.1 | Glasses synthesis

Three glass compositions based on SiO_2–Na_2O–CaO–P_2O_5 were studied, a parent glass[24] and two other glasses with the incorporation of 2.5% (wt%) of Gd_2O_3 or Yb_2O_3. The theoretical compositions of glasses are presented in Table 1. For the synthesis, oxides were used as precursors and glasses were melted in a platinum crucible at 1600°C, for 1 hour. After cooling, the glasses were crushed and sieved to obtain particles with a diameter less than 125 μm. The particle size of the glasses was measured by performing measurements using a CILAS 1190 laser particle size analyzer (CILAS, USA).

2.2 | Dissolution test

The dissolution test was performed following the recommendation of the ISO 1093-14 standard. In brief, a tris-buffer solution prepared with 13.25 g of (Hydroxymethyl) aminomethane (Tris) per liter of ultrapure water, and pH adjusted for 7.4 with 1 mol/L HCl at 37°C, was used as dissolution medium.[25,26] In order to perform the test, 75 mg of each glass was immersed into 1.5 mL of Tris-buffer solution, and placed in an orbital shaker for periods of 1, 6, 12, 24, 72, 120, and 168 hours. The concentration of ions released from glass was measured by inductively coupled plasma optical emission spectrometry model with axial vision series 710 (Varian), using the emission lines: Si ($\lambda = 250.690$ nm), Na ($\lambda = 588.995$ nm), P ($\lambda = 213.618$ nm), Ca ($\lambda = 422.673$ nm), Gd ($\lambda = 342.246$ nm), and Yb ($\lambda = 328.937$ nm).

2.3 | Bioactivity behavior test

The bioactivity behavior test was performed using simulated body fluid (SBF) solution following the recommendation of the TC04 of the International Commission on Glass.[27] The preparation of the SBF solution was described elsewhere.[28] For the test, 4.17 mg of glass powder was immersed into 100 mL of SBF solution, and placed in a shaker for periods

TABLE 1 Theoretical compositions of studied glasses (wt%)

Compositions	SiO_2	Na_2O	CaO	P_2O_5	Gd_2O_3	Yb_2O_3
BG	47.28	31.39	15.33	6.00	—	—
BG–Gd	46.10	30.60	14.95	5.85	2.5	—
BG–Yb	46.10	30.60	14.95	5.85	—	2.5

of 1, 3, 5, and 7 days. The concentration of ions released from the glass was determined using the same parameters mentioned in section 2.22.2.

After each experimental periods immersed in SBF, glass powders were filtered, rinsed with acetone to terminate any ongoing reactions, and analyzed by scanning electron microscopy (SEM) coupled with energy-dispersive X-ray analysis (EDS), X-ray diffraction (XRD), and Fourier transform infrared spectrometry (FTIR) in order to identify morphological, structural, and functional groups changes on glass surface, respectively. SEM_EDS analysis was performed in an electronic microscope model JSM-6010LA (JEOL, USA), and before analysis glass powders were coated with carbon by sputtering. XRD was conducted in diffractometer D8 Focus (Bruker AXS, USA) using CuK_α radiation ($\lambda = 0.15406$ nm) in the range of $10° < 2\theta < 70°$ and step size of 0.024°/s. FTIR spectra were collected in a spectrometer Spectrum Two (Perkin Elmer, USA) over 700-4000 cm^{-1} range.

2.4 | Cytotoxicity test

Biological characterization of glasses was performed by the indirect method. Conditioned medium was obtained by immersion of glass powder in cell culture medium (DMEM low glucose, with 10% bovine serum and 1% penicillin),[29] and placed in a cell incubator for 48 hours (37°C-5% CO_2). Then, the solutions were filtered and diluted in different concentrations (100%; 50%; 25%; 12.5%, and 6.25%). Mesenchymal stem cells derived from deciduous teeth (SHEDs) were placed on 96-well plaques at a concentration of 10^3 cells/well, using regular culture medium, and maintained in a cell incubator for 24 hours. Then, the cell culture medium was replaced by the conditioned medium in different concentrations, and the plaques with cell culture were placed in a cell incubator for 72 hours (37°C-5% CO_2). The cell viability, after this period, was determined using MTT reduction assay.[29,30]

3 | RESULTS

The powder particle size of each glass is presented in Figure 1, and the values of particle size diameter at 10%, 50%, and 90%, and the particle size distribution are shown in Table 2. It was noted that all the glass particles ranges from 0.3 to 125 μm. The compositions BG and BG-Yb showed mean particle size ~72 μm, while the composition BG–Gd glass showed the smallest mean particle size (~55 μm).

The ionic concentration of Si, Na, Ca, and P released from glass particles in Tris-HCl buffer solution are shown in Figure 2. Regarding silicon behavior, in the first 24 hours, glass dissolution showed a non-linear trend, which was named as K_1 regime. After 24 hours, glass dissolution presents a linear behavior, characterized by a dissolution kinetics K_2. The highlighted areas in Figure 2 show the K_1 (1a) and K_2 (2c) regimes. Sodium concentration follows the same kinetic trend as silicon (Figure 2D,E). However, the analysis of calcium and phosphorous concentration did not follow the same kinetics of silicon, once these ions undergo precipitation reactions during the dissolution experiments (Figure 2E,F). The incorporation of gadolinium and ytterbium in the glasses structure changed silicon dissolution kinetics, mainly in the K_2 regime. In such regime, the incorporation rare earths decreased silicon release from 11.63 μg/mL·h for BG to 6.78 μg/mL·h and near to 0.0 μg/mL·h for BG–Yb and BG–Gd, respectively (Figure 2B). Similar tendency was observed in sodium release (Figure 2C).

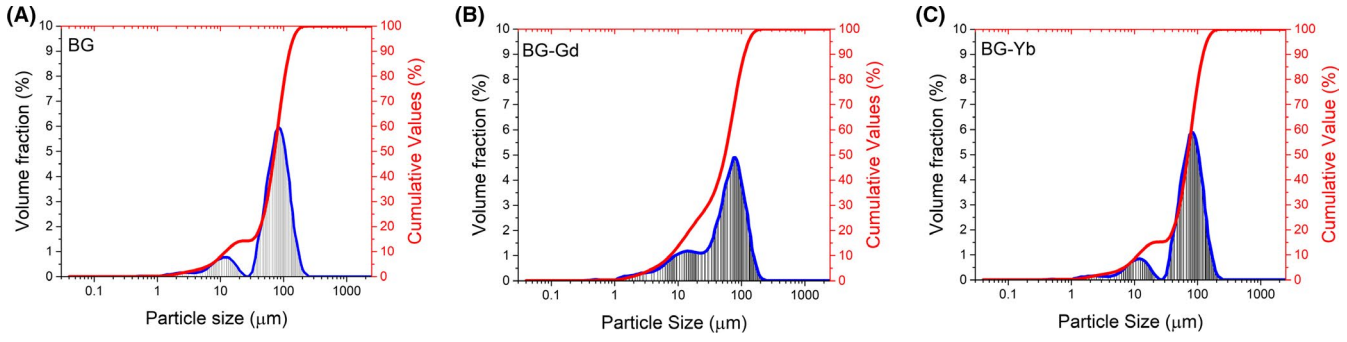

FIGURE 1 Particle size distribution of glass powders (A) BG, (B) BG–Gd, (C) BG–Yb [Colour figure can be viewed at wileyonlinelibrary.com]

	Diameter at 10%	Diameter at 50%	Diameter at 90%	Mean Diameter
BG	11.76 ± 0.26	71.65 ± 0.98	124.64 ± 00.56	72.78 ± 1.07
BG-Gd	7.68 ± 0.43	55.14 ± 0.30	111.33 ± 0.18	57.51 ± 0.31
BG-Yb	10.79 ± 0.61	69.03 ± 1.01	121.833 ± 0.57	70.18 ± 1.09

TABLE 2 Values related to particle size distribution of BG, BG–Gd, and BG–Yb glasses

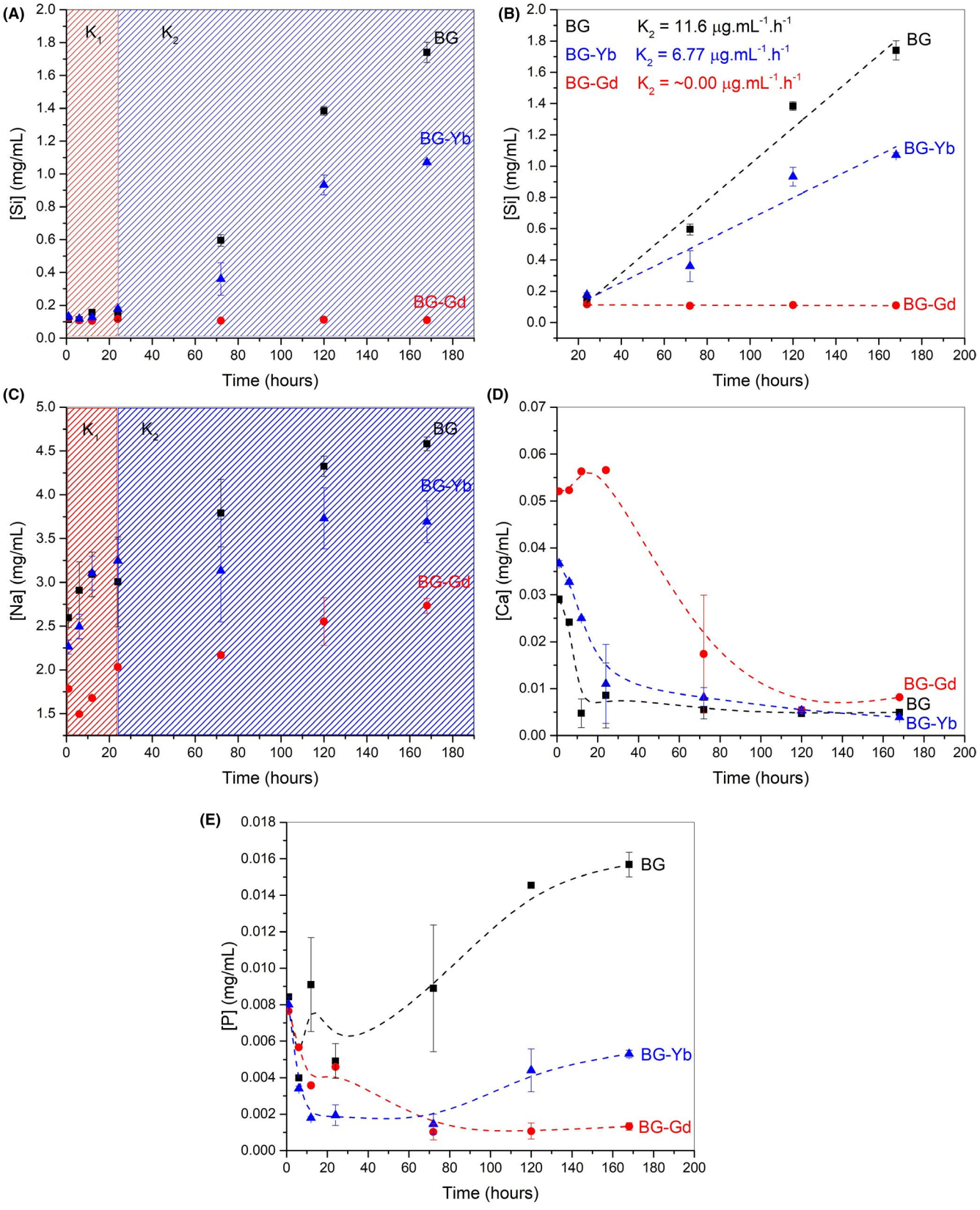

FIGURE 2 Si, Na, Ca, and P concentration as a function of immersion time in Tris-HCl. In (A) and (C) areas of K_1 and K_2 of silicon and sodium, respectively. In (B) highlighting the points of K_2 regime of silicon. Dissolution trends of calcium and phosphorous is presented in (D) and (E), respectively [Colour figure can be viewed at wileyonlinelibrary.com]

The glass-derived ionic products were also monitored in SBF solution in order to compare with data obtained in TRIS-HCl, and the concentration of the dissolution products of the studied glasses is shown in Figure 3A-D for the based-glass elements. Figure 3E,F show the concentration of Gd and Yb in BG–Gd and BG–Yb, respectively.

Regarding silicon concentration (Figure 3A), a quicker dissolution was noted on the first day, followed by a reduced dissolution rate for more extended periods. Similar behavior was observed for all glasses. About sodium release (Figure 3B), BG glass showed a continuous release over time, while BG–Gd and BG–Yb glasses showed a nearly constant release. On the other hand, calcium and phosphorous release behave differently. Calcium concentration (Figure 3C) has an initial increase followed by a decrease in concentration.

Interestingly, the decrease in calcium concentration occurs after three days for BG glass and after only one day for rare earth-containing glasses. Comparable behavior was observed in phosphorous concentration (Figure 3D), that is, an increase in concentration followed by a decrease. For BG glasses, the decrease in phosphorous concentration was noted after five days soaked in SBF solution, and in rare earth-containing glasses, such decrease was noticed right on the first day. The release of gadolinium and ytterbium from rare earth-containing glasses (Figure 3D,E) was deficient, which might be related to a shallow concentration of such elements in SBF solution after different periods.

Figure 4 presents the surface morphology and EDS spectra of glass surface before and after 7 days immersed in SBF solution for all studied glasses. Figure 5 shows the EDS composition mapping of BG, BG–Gd, and BG–Yb glasses, respectively, where calcium, sodium, phosphorus, and silicon were mapped. The SEM micrographies and EDS spectra for other periods of immersion in SBF other than 7 days can be checked in the Figures S1, S2, S3, and S4.

The immersion of these glasses in SBF solution changed their surface morphologies, which are related to an amorphous calcium phosphate layer formation. In Figure S1, S2, and S3 it is noted that changes in morphology caused by the precipitation of calcium phosphate on the glass surface is observed in different kinetics for rare earth-containing glass and its parent glass. In BG glass (Figure 4A,D, and Figure S1), these differences in morphology are more evident after three days of immersion in SBF. On the other hand, in BG–Gd (Figure 4B,E, and Figure S2) and BG–Yb (Figure 4C,F, and Figure S3) glasses, these differences can be observed after one day immersed in SBF solution, indicating a quicker calcium phosphate deposition. Such difference in morphologies was also noted in the EDS spectra (all the details in Figure 4, S1, S2, and S3) and chemical element mapping images (Figure 5 and Figure S4), which shows a decrease in intensity of silicon and sodium, and an increase in the intensity of calcium and phosphorous for rare earth-containing glasses.

XRD patterns before and after bioactivity experiments are shown in Figure 6. Before immersion in SBF solution (Figure 6A), XRD results were typical of glassy materials, showing broadband between 24° and 36°, and did not exhibit any crystalline peaks. After immersion in SBF for seven days, some characteristic peaks of an calcium phosphate phase were observed at 26 and 32° (Figure 6B-D), which are often related to the conversion of the amorphous calcium phosphate into hydroxyapatite. However, the absence of a typically crystalline pattern suggests that this calcium phosphate phase grown on the glass surface was not fully crystallized.

Figure 7A-C shows FTIR spectra of studied glasses before and after different periods soaked in SBF solution. Initial characterization of these glasses showed that all of them presented the same functional groups, ie, structural SiO_2 (800 cm^{-1}), Q^1 (850 cm^{-1}), Q^2 (950 cm^{-1}), Si–O-Metal (1050 cm^{-1}), Q^3 (1100 cm^{-1}), and Q^4 (1200 cm^{-1}).[31–34] After immersion in SBF solution, all spectra predominantly showed a contribution of phosphate (PO_4) groups (960, 1000, and 1040 cm^{-1})[35] in the overall spectra. Notably, after one day in SBF solution, the FTIR spectra of all glasses showed a combination of silicates and phosphate functional groups, while after three days in SBF solution, the FTIR spectra shifts for a dominant phosphate functional group. Interestingly, for rare earth-containing glasses, after one day phosphate functional groups of FTIR spectra are more intense than in the BG glass, suggesting a faster phosphate deposition in rare earth-containing glasses.

The results of the cytotoxicity behavior are shown in Figure 8. All studied glasses presented cell viability higher than 80%, being considered non-cytotoxic in any concentration of the conditioned medium. The proliferation of the SHED cells increased with the decrease of conditioned medium concentration, indicating that viability is dose-dependent. The behavior of all samples was similar, and when the different glasses are compared, no statistical difference was noted.

4 | DISCUSSION

Initial characterization of the glass powders included the measurement of particle size distribution. Our results showed that the BG and BG–Yb glasses have the same main particle diameter, while the BG–Gd glass has a smaller size. However, we considered that such difference was not that significant to affect the dissolution results, considering that all the glasses showed similar particle size distribution and range (from 0.03 to 125 μm). Therefore, we propose that all our finds discussed hereinafter are more influenced by glass composition rather than any effect related to particle size or surface area.

Usually, the dissolution kinetics of multicomponent glasses is studied considering that the dissolution kinetics relies upon

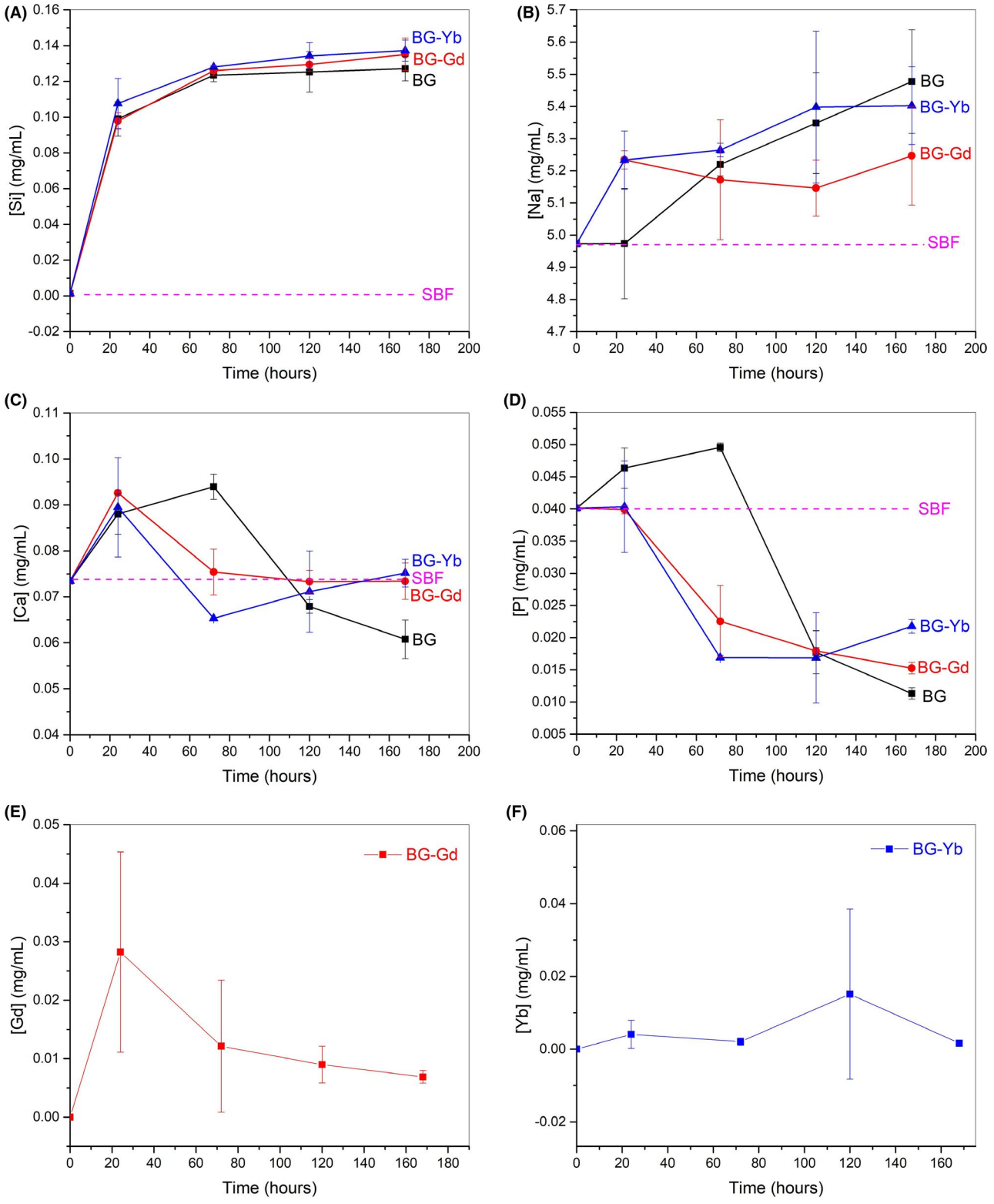

FIGURE 3 Elementary concentration of (A) silicon, (B) sodium, (C) calcium, (D) phosphorus from BG, BG-Gd, and BG-Yb glasses, and release of (E) Gadolinium and (F) Ytterbium from BG-Gd and BG-Yb, respectively [Colour figure can be viewed at wileyonlinelibrary.com]

the glass former species, once the break of bridging oxygen bonds requires more energy than breaking the bonds between glass modifiers and non-bridging oxygens,[36–39] or even the energy needed for ionic percolation in the glass structure.[40] Therefore, we established some assumption to be considered during the understanding of our results: (a) Since we have silicate-based glasses, it was considered that cleavage of Si–O–Si bonds was the limiting-step of glass dissolution. Therefore,

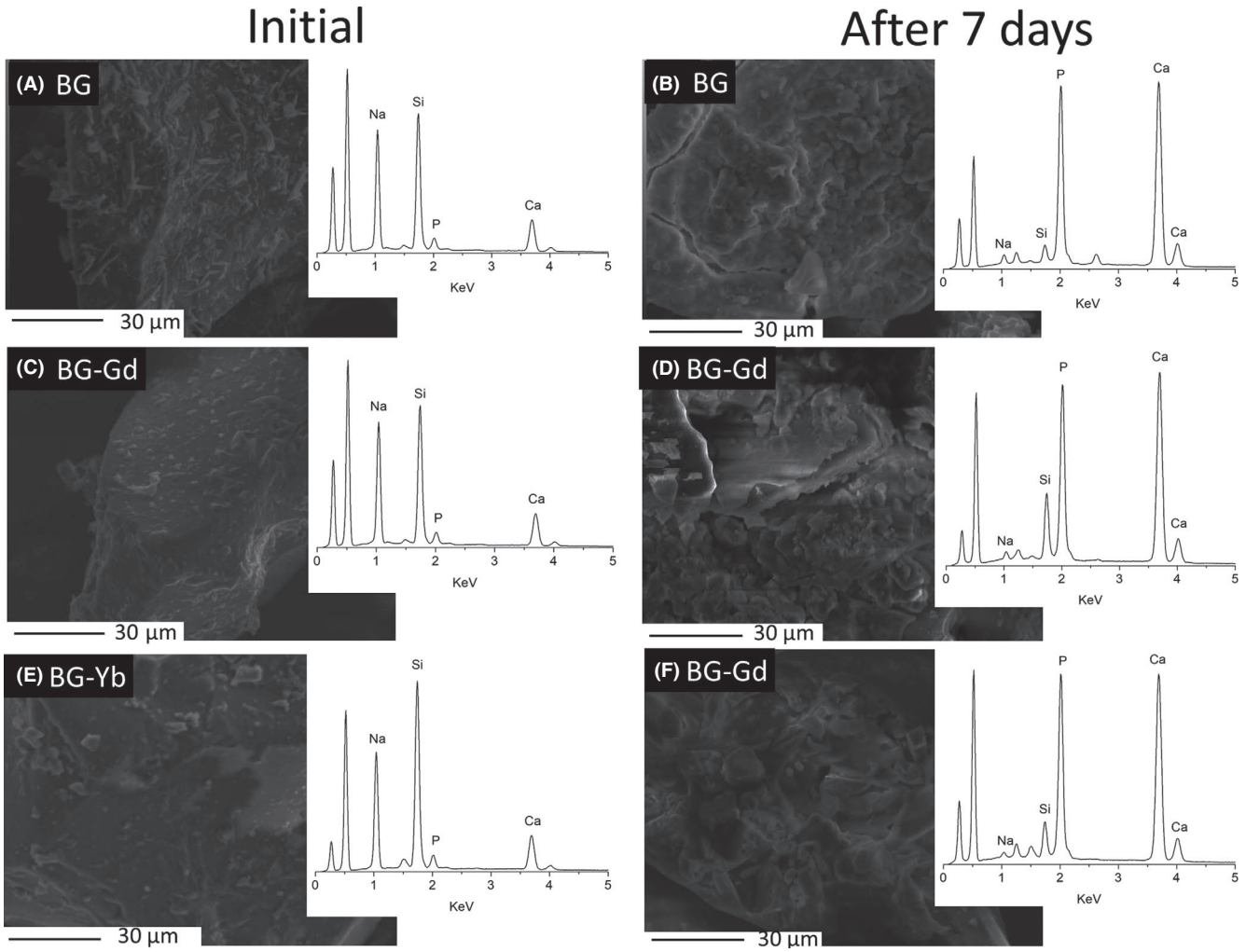

FIGURE 4 Scanning electron micrographies and energy dispersive spectra (in detail) of all glasses before (A-C) and after 7 d immersed in SBF solution (D-F)

glass dissolution kinetics of our glasses was firstly based on the analysis of silicon concentration[41]; (b) we understood sodium leaching as a percolation phenomenon, considering that sodium has a higher mobility in glass structure than other ions[20,37,40]; (c) dissolution kinetics constants cannot be attributed to calcium and phosphate ions, once these ions undergo precipitation reactions during the dissolution test.

Therefore, the dissolution behavior of bioactive glasses in aqueous media was divided into two stages, named K_1 and K_2, respectively. In the first stage (K_1), such process is dominated by the exchange of alkali ions with protons in solution in which the dissolution rate varies with the square root of time. It is noteworthy to mention that in the first hour, silicon dissolution varies from zero to 135 mg/mL, and such concentration remained almost constant up to 24 hours of experiment. From our point of view, in the first hour the dissolution rate was very quick because the dissolution rate was governed only by surface reaction mechanism. After one hour, there was the formation of a hydrated layer which slowed down the dissolution rate, as well as promoted the precipitation of calcium and phosphate ions, which led to a near zero dissolution. All these steps are well reported in the literature,[25,39] and they are used as a general dissolution theory of glasses. The formation of the calcium phosphate layer was observed by the decrease in calcium and phosphate concentration in the first 24 hours of experiment, suggesting the precipitation of these elements onto glass surface.

In the second stage (K_2), the network dissolution is the primary mechanism, and silicon concentration is linear-dependent with time.[42] Thus, in the studied glasses, it can be observed that the first stage occurred within the first 24 hours and later the second stage takes place. As observed in the K_2 regime (Figure 2B), the dissolution of the glasses was more affected by incorporation of rare earth elements, resulting in a diminished release of silicon and sodium ions, in both rare earth-containing glasses. Also, the dissolution rate was slower for gadolinium than ytterbium glasses, which can be related to the larger atomic radius of gadolinium due to the occurrence of the lanthanide contraction.

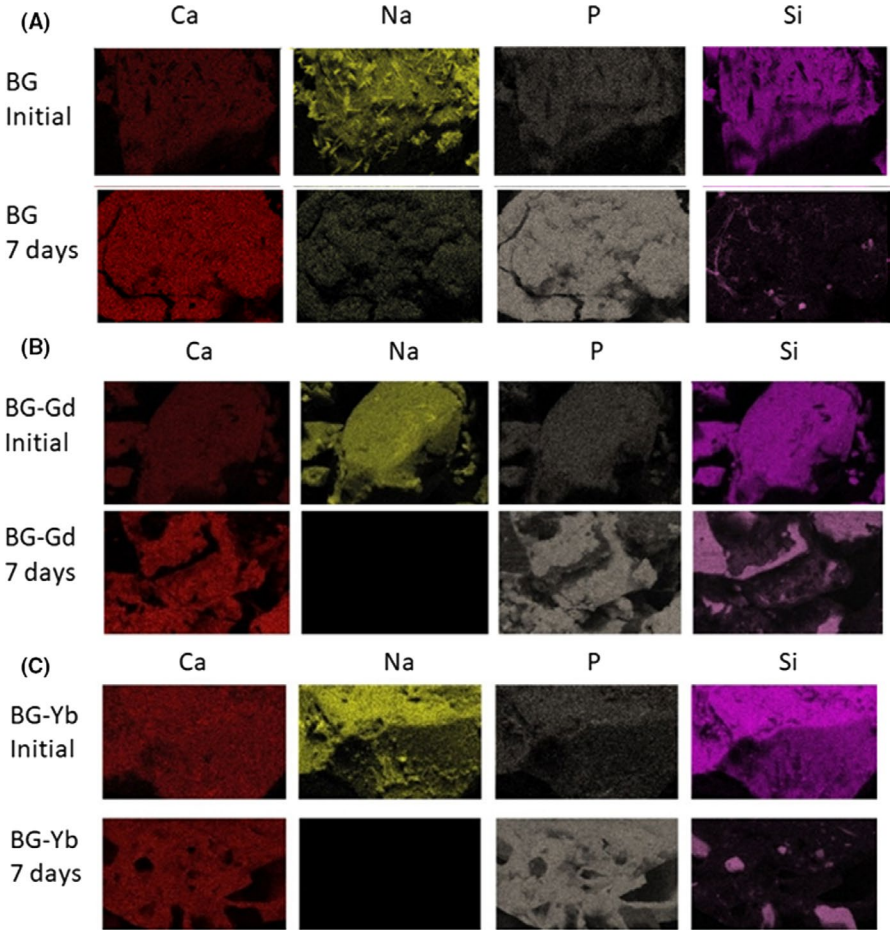

FIGURE 5 Energy dispersive elementary mapping of glasses before and after 7 d immersed in SBF solution. BG (A), BG–Gd (B), and BG–Yb (C). The elements mapped were: calcium (red), sodium (yellow), phosphorous (gray), and silicon (purple) [Colour figure can be viewed at wileyonlinelibrary.com]

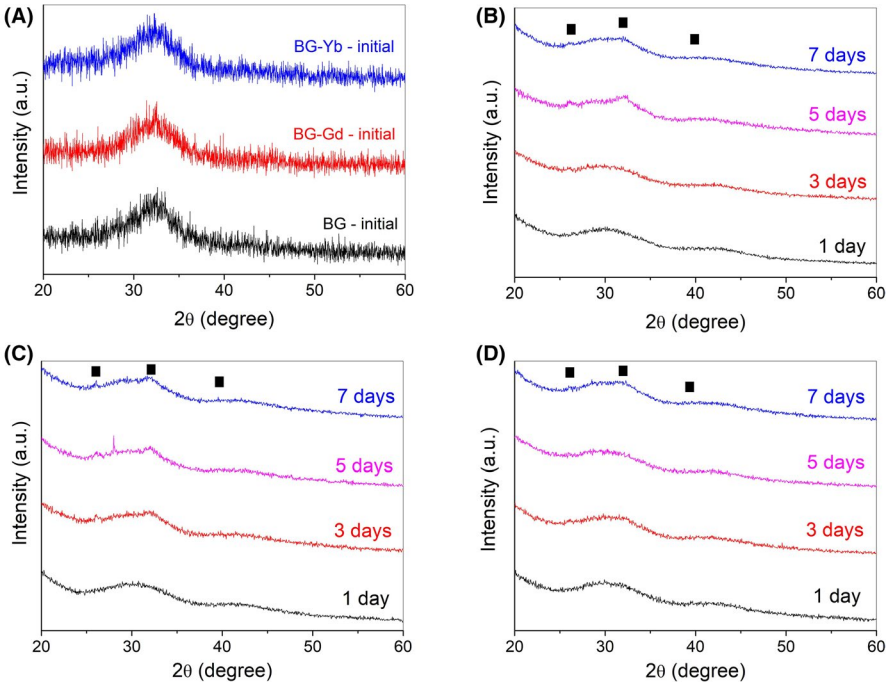

FIGURE 6 258699071628000X-ray diffraction of the glass powders soaked in SBF solution: (A) glass powders before the bioactivity test; BG (B), BG–Gd (C), and BG–Yb (D) glasses after different periods soaked in SBF solution. • calcium phosphate phase [Colour figure can be viewed at wileyonlinelibrary.com]

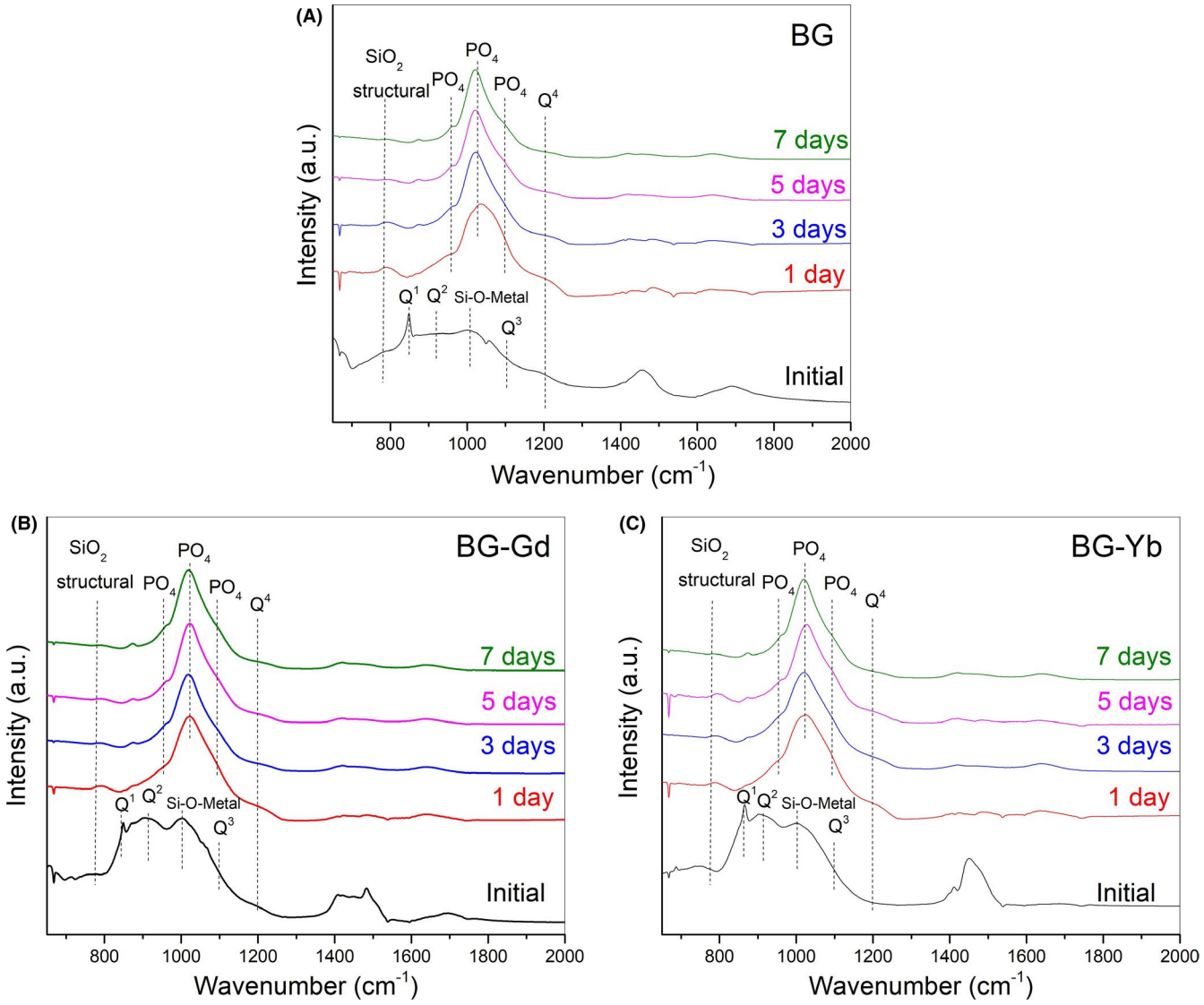

FIGURE 7 Fourier transform infrared spectra of (A) BG, (B) BG–Gd, and (C) BG–Yb glasses before and after different periods immersed in SBF solution [Colour figure can be viewed at wileyonlinelibrary.com]

The decrease in glass dissolution as rare earth is added in the structure also suggests that rare earth establish stronger chemical bonds with oxygens than calcium and sodium. In a previous work,[21] we showed that gadolinium and ytterbium has an intermediate ionic role in the glass structure, being found either as glass modifier or glass former, which also matches with computational simulations carried out by other researchers.[15,16] Therefore, considering the existence of Si–O–RE bonds, where RE act as a glass former, we can infer that such bonds are stronger than Si–O–Si, which resulted in a slower glass dissolution rate. In fact, after theoretically modeling the structure of bioactive glasses containing yttrium, Christie and Tilocca[15,16,43] have already pointed out that Si–O–RE bonds could be stronger, which could lead to changes glass dissolution, and then affect bioactivity behavior. Thus, our experimental finds not only confirms that Si–O–RE bonds are stronger than Si–O–Si but also assured that such decreased dissolution kinetics did not affect bioactivity, as further discussed hereinafter.

The incorporation of rare earth elements also influenced sodium release. These rare earth-containing glasses showed a reduced sodium release rate when compared with the BG parent glass. Differently of silicon, whose dissolution depends on cleavage of Si-O-Si bonds, sodium release occurs by percolation in the glass structure.[40] In such mechanism, sodium diffuses in the glass structure by hopping, and the neighbor atoms influence its mobility. In according to Tilocca,[40] in 45S5 bioactive glasses, sodium migration depends on temporary calcium displacement in the glass structure in a backward-forward movement, enabling sodium ions to move to this temporary calcium-vacated site, also opening a pathway for sodium movement. Consequently, the reduced sodium release in rare earth-containing glasses suggests that gadolinium and ytterbium

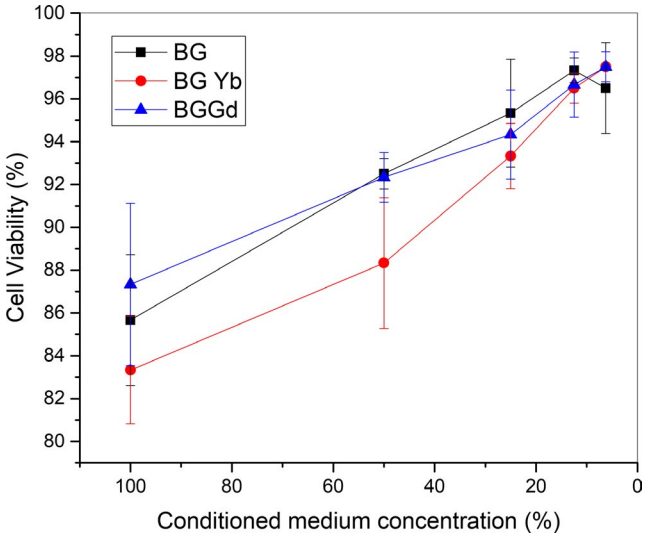

FIGURE 8 SHED cell viability in function of different concentrations of the conditioned medium containing dissolution products of BG, BG–Gd, and BG–Yb glasses [Colour figure can be viewed at wileyonlinelibrary.com]

are diminishing sodium mobility in the glass structure. Considering that fraction of rare earth ions acts as modifier ions in the glass structure, gadolinium and ytterbium are hiding sodium migration because of their larger atomic radius compared to calcium, which could affect their backward-forward movement.

It is important to mention that the ionic concentration observed in this work in the Figures 1 and 2 are in the same order of magnitude of other works available in the literature.[42,44] However, the Si, Ca, P, and Na concentration are higher in this work, which we addressed to our glass composition, which differs from the 45S5 bioactive glass composition due to its higher content of Na. Because of such higher Na concentration, our glass exhibit higher glass dissolution kinetics, leading to higher ionic release.

As mentioned previously, although glass dissolution was affected by rare earth incorporation, we did not observe any adverse effect of such incorporation on bioactivity behavior of our glasses. Instead, bioactivity behavior was favored in rare earth-containing glasses. The causes of such different behavior between SBF and TRIS-HCl solution have been attributed to solution ionic strength and supersaturation.[45–47] Indeed, SBF has much more ions dissolved, thus being more saturated and prone to precipitation reactions.[28] Besides, silicon concentration in SBF is at least ten times lower than in TRIS-HCl solution, indicating that the ionic strength of SBF solution has slowed glass dissolution, and the effect of rare earth on glass dissolution is not pronounced. Additionally, the plateau in silicon concentration observed in Figure 3A is related to the formation of a calcium phosphate layer on the glass surface, which acts as a passivation layer impeding further water corrosion.

The deposition of calcium phosphate on glasses surface during bioactivity test was observed in the XRD, EDS, and FTIR results. The XRD results indicate the presence of only showed the presence of a calcium phosphate phase deposited on the glass surface as an initial crystalline array. The EDS results showed that more calcium and phosphorous are found on the glass surface in the expense of silicon and sodium, in a time-dependent manner. However, XRD and EDS did not show an evident influence of rare earth elements on glass bioactivity.

In contrast, the FTIR results showed valuable findings. After one day, all the samples presented phosphate functional groups, suggesting that even in 24 hours bioactivity was evidenced in the glasses. Nevertheless, rare earth-containing glasses seem to present a significant contribution from phosphates than the parent glass, which suggests that phosphate precipitation was instead promoted in the glasses containing rare earth. Indeed, the ICP-OES showed that in rare earth-containing glasses the precipitation of phosphorous and calcium begins earlier than in BG glass, which was observed by a decrease in concentration of such elements. Thus, FTIR and ICP-OES results suggest that gadolinium and ytterbium favored bioactivity behavior of glasses.

The literature[17,19,48,49] have shown that cerium did not alter bioactivity behavior when present in glass composition at low concentrations, which is in agreement with our results—however, none of them shown that low concentrations of rare earth could promote bioactivity. According to Borges et al,[21] the incorporation of rare earth elements (Gd and Yb) in the glass structure results in an increase of non-bridging oxygens despite their intermediate role in the glass structure, leading to a less connected glass network. Probably, these less connected network alters the release of calcium and phosphate species, which favored bioactivity behavior.

Regarding cytotoxicity test, all studied glasses did not present toxicity in any concentration, suggesting their potential use in in vivo applications. Following the literature,[50,51] the cytotoxicity of rare earth elements increases from lutetium to lanthanum, which means that ytterbium is less cytotoxic than gadolinium. Besides, studies carried out with macrophages showed that loads up to 80 mg/mL of ytterbium oxide did not induce significant cytotoxicity response.[50] Considering the low concentration of ytterbium and gadolinium in our glasses, possibly the amount of rare earth released was not enough to reach a minimal cytotoxic effect. In overall, all the results suggest that these rare earth-containing glasses are suitable materials for biomedical applications.

5 | CONCLUSIONS

In this work, rare earth-containing bioactive glasses based on the SiO_2–Na_2O–CaO–P_2O_5–RE_2O_3 (RE = Gd or Yb) were obtained by melting-quenching. The dissolution experiments

showed that rare earth led to a decrease in glass dissolution due to the more covalent character of Si–O–RE bonds related to part of rare earth that act as glass former in the glass structure. However, when the glasses were soaked in SBF solution, this behavior was not pronounced due to the higher ionic strength of SBF. Also, Gd and Yb elements promoted calcium phosphate deposition on the glass surface, suggesting a possible higher bioactivity character of such rare earth-containing glasses. Cytotoxicity test showed that all the glass were biocompatible, being the viability dose-dependent. The overall results suggested that these glasses are promising materials for biomedical applications.

ACKNOWLEDGMENTS

The authors are grateful to the Multiuser Central Facilities (CEM-UFABC) and labs 507-3 and 712-3 from UFABC for facilities support, and MSc. Asaph and Prof. Dr. Marcia Ap. Spinacé for the technical support in FTIR analyses. The author also thanks FAPESP, CNPq, and CAPES for financial support.

ORCID


Juliana Marchi https://orcid.org/0000-0002-0663-0463

REFERENCES

1. Cornejo CR. Luminescence in rare earth ion-doped oxide compounds. In: Thirumalai J editor. Luminescence - an outlook on the phenomena and their applications (1st ed.). IntechOpen;2016:33–63. [cited 2018 Nov 1]. Available from https://www.intechopen.com/books/luminescence-an-outlook-on-the-phenomena-and-their-applications/luminescence-in-rare-earth-ion-doped-oxide-compounds
2. Loft SM, Coles IP, Dale RG. The potential of ytterbium 169 in brachytherapy: a brief physical and radiobiological assessment. Br J Radiol. 1992;65(771):252–7.
3. Sadeghi M, Taghdiri F, Hosseini SH, Tenreiro C, Tenreiro C. Monte Carlo calculated TG-60 dosimetry parameters for the β-emitter S 153 m brachytherapy source Monte Carlo calculated TG-60 dosimetry parameters for the β-emitter Sm brachytherapy source. Med Phys. 2010;5370(37):5369–95.
4. Hosseini SH, Enferadi M, Sadeghi M. Dosimetric aspects of Ho brachytherapy biodegradable glass seed. Appl Radiat Isot. 2013;73:109–15.
5. Dahiya M. Brachytherapy: a review. J Crit Rev [Internet]. 2016;3(2):6–10. Available from http://innovareacademics.in/journals/index.php/jcr/article/view/10183.
6. Marchi J. Biocompatible glasses: from bone regeneration to cancer treatment, 1st ed. Marchi J, editor. Cham, Switzerland: Springer International Publishing; 2016.
7. Hoppe A, Mourino V, Boccaccini AR. Therapeutic inorganic ions in bioactive glasses to enhance bone formation and beyond. Biomater Sci. 2013;1(3):254–6.
8. Hoppe A, Güldal NS, Boccaccini AR. Biomaterials: a review of the biological response to ionic dissolution products from bioactive glasses and glass-ceramics. Biomaterials. 2011;32(11):2757–74.
9. Zanotto ED, Coutinho F. How many non-crystalline solids can be made from all the elements of the periodic table? J Non Cryst Solids. 2004;347(1–3):285–8.
10. Roberto WS, Pereira MM, Campos T. Structure and dosimetric analysis of biodegradable glasses for prostate cancer treatment. Artif Organs. 2003;27(5):432–6.
11. Roberto WS, Pereira MM, Campos T. Dosimetric analysis and characterization of Radioactive seeds produced by the sol-gel method. Key Eng Mater. 2003;242:579–82.
12. Khorshidi A, Ahmadinejad M, Hosseini SH, N-particle C. Evaluation of a proposed biodegradable 188 Re source for brachytherapy application: a review of dosimetric parameters. Medicine (Baltimore). 2015;94(28):1–7.
13. Taghdiri F, Sadeghi M, Hosseini SH, Athari M. TG-60 dosimetry parameters calculation for the β - emitter 153 Sm brachytherapy source using MCNP. Iran J Radiat Res. 2011;9(2):103–8.
14. Aspasio RD, Borges R, Marchi J. Biocompatible glasses for cancer treatment. In: Marchi J editor. Biocompatible glasses: from bone regeenration to cancer treatment [Internet], 1st ed. Switzerland: Springer International, 2016; pp. 249–65. Available from: http://link.springer.com/10.1007/978-3-319-44249-5.
15. Christie JK, Malik J, Tilocca A. Bioactive glasses as potential radioisotope vectors for in situ cancer therapy: investigating the structural effects of yttrium. Phys Chem Chem Phys. 2011;13(39):17749–55.
16. Christie JK, Tilocca A. Integrating biological activity into radioisotope vectors: molecular dynamics models of yttrium-doped bioactive glasses. J Mater Chem. 2012;22:12023–31.
17. Leonelli C, Lusvardi G, Malavasi G, Menabue L, Tonelli M. Synthesis and characterization of cerium-doped glasses and in vitro evaluation of bioactivity. J Non Cryst Solids. 2003;316(2–3):198–216.
18. Nicolini V, Varini E, Malavasi G, Menabue L, Menziani MC, Lusvardi G, et al. The effect of composition on structural, thermal, redox and bioactive properties of Ce-containing glasses. Mater Des [Internet]. 2016;97:73–85.
19. Salinas AJ, Shruti S, Malavasi G, Menabue L, Vallet-Regí M, Malavasi G, et al. Substitutions of cerium, gallium and zinc in ordered mesoporous bioactive glasses. Acta Biomater. 2011;7(9):3452–8.
20. Pedone A, Charpentier T, Malavasi G, Menziani MC. New insights into the atomic structure of 45S5 bioglass by means of solid-state NMR spectroscopy and accurate first-principles simulations. Chem Mater. 2010;22(19):5644–52.
21. Borges R, Schneider JF, Marchi J. Structural characterization of biocompatible glasses containing rare earth elements (Gd and/or Yb). J Mater Sci. 2019;54(17):11390–9.
22. Hu F, Wei X, Qin Y, Jiang S, Li X, Zhou S, et al. Yb^{3+}/Tb^{3+} co-doped $GdPO_4$ transparent magnetic glass-ceramics for spectral conversion. J Alloys Compd. 2016;674:162–7.
23. Saxena SK, Kumar Y, Jagadeesan KC, Nuwad J, Bamankar YR, Dash A. Studies on the development of 169Yb-brachytherapy seeds: new generation brachytherapy sources for the management of cancer. Appl Radiat Isot. 2015;101:75–82.
24. Borges R, da Silva AC, Marchi J. Evaluation of the bioactivity behavior of a 48 wt%SiO_2 bioglass through experiments in simulated body fluid. Mater Sci Forum. 2012;727–728:1238–42.

25. Fagerlund S, Ek P, Hupa L, Hupa M. Dissolution kinetics of a bioactive glass by continuous measurement. J Am Ceram Soc. 2012;95(10):3130–7.
26. International Standard Organization. Biological evaluation of medical devices Part 14: Identification and quantification of degradation products from ceramics (ISO Standards no. 10933-14:2001). 2001 [cited 2019 Mar 5]. Available from https://www.iso.org/standard/22693.html
27. Maçon A, Kim TB, Valliant EM, Goetschius K, Brow RK, Day DE, et al. A unified in vitro evaluation for apatite-forming ability of bioactive glasses and their variants. J Mater Sci Mater Med. 2015;25(2):115.
28. Kokubo T, Takadama H. How useful is SBF in predicting in vivo bone bioactivity? Biomaterials. 2006;27(15):2907–15.
29. Lopez T, Diniz I, Ferreira LS, Marchi J, Borges R, de Cara S, et al. Bioactive glass plus laser phototherapy as promise candidates for dentine hypersensitivity treatment. J Biomed Mater Res - Part B Appl Biomater. 2017;105(1):107–16.
30. Marchi J, Ribeiro C, Bressiani AHdA, Marques MM. Cell response of calcium phosphate based ceramics, a bone substitute material. Mater Res [Internet]. 2013;16(4):703–12. Available from: http://www.scielo.br/scielo.php?script=sci_arttext&pxmlid=S1516-14392013000400003&lng=en&tlng=en
31. Macdonald SA, Schardt CR, Masiello DJ, Simmons JH. Dispersion analysis of FTIR re¯ection measurements in silicate glasses. J Non Cryst Solids. 2000;275:72–82.
32. Serra J, González P, Liste S, Serra C, Chiussi S, León B, et al. FTIR and XPS studies of bioactive silica based glasses. J Non Cryst Solids. 2003;332(1–3):20–7.
33. Aguiar H, Serra J, González P, León B. Structural study of sol–gel silicate glasses by IR and Raman spectroscopies. J Non-Crystalline Solids. 2009;355(8):475–80. http://sci-hub.tw/10.1016/j.jnoncrysol.2009.01.010.
34. Serra J, González P, Liste S, Chiussi S, León B, Pérez-Amor M, et al. Influence of the non-bridging oxygen groups on the bioactivity of silicate glasses. J Mater Sci Mater Med. 2002;13(12):1221–5.
35. Berzina-Cimdina L, Borodajenko N. Research of calcium phosphates using fourier transform infrared spectroscopy. In: Theophile Th, editor. Infrared spectroscopy - materials science, engineering and technology [Internet], 1st ed. Rijeka: Intech, 2012; pp. 121–48. Available from: http://www.intechopen.com/books/infrared-spectroscopy-materials-science-engineering-and-technology/research-of-calcium-phosphates-using-fourier-transformation-infrared-spectroscopy.
36. Bunker BC, Arnold GW, Wilder JA. Phosphate glass dissolution in aqueous solutions. J Non Cryst Solids. 1984;64(3):291–316.
37. Christie JK, Ainsworth RI, de Leeuw NH. Investigating structural features which control the dissolution of bioactive phosphate glasses: beyond the network connectivity. J Non-Crystall Solids. 2016;432:31–4.
38. Kagan M, Lockwood GK, Garofalini SH. Correction: reactive simulations of the activation barrier to dissolution of amorphous silica in water. Phys Chem Chem Phys. 2014;16(46):25649–25649.
39. Oelkers EH. General kinetic description of multioxide silicate mineral and glass dissolution. Geochim Cosmochim Acta. 2001;65(21):3703–19.
40. Tilocca A. Sodium migration pathways in multicomponent silicate glasses: Car-Parrinello molecular dynamics simulations. J Chem Phys. 2010;133(1):014701.
41. Singh RK, Srinivasan A. Applied surface science bioactivity of SiO_2–CaO–P_2O_5–Na_2O glasses containing zinc-iron oxide. Appl Surf Sci. 2010;256:1725–30.
42. Cerruti MG, Greenspan D, Powers K. An analytical model for the dissolution of different particle size samples of Bioglass® in TRIS-buffered solution. Biomaterials. 2005;26(24):4903–11.
43. Tilocca A. Realistic models of bioactive glass radioisotope vectors in practical conditions: structural effects of ion exchange. J Phys Chem C. 2015;119:17442–27448.
44. Sepulveda P, Jones JR, Hench LL. Characterization of melt-derived 45S5 and sol-gel–derived 58S bioactive glasses. J Biomed Mater Res. 2001;58(6):734–40.
45. Shah FA, Brauer DS, Wilson RM, Hill RG, Hing KA. Influence of cell culture medium composition on in vitro dissolution behavior of a fluoride-containing bioactive glass. J Biomed Mater Res - Part A. 2014;102(3):647–54.
46. Kirste G, Brandt-Slowik J, Bocker C, Steinert M, Geiss R, Brauer DS. Effect of chloride ions in Tris buffer solution on bioactive glass apatite mineralization. Int J Appl Glas Sci. 2017;8(4):438–49.
47. Sakai S, Anada T, Tsuchiya K, Yamazaki H, Margolis HC, Suzuki O. Comparative study on the resorbability and dissolution behavior of octacalcium phosphate, β-tricalcium phosphate, and hydroxyapatite under physiological conditions. Dent Mater J [Internet]. 2016;35(2):216–24. https://www.jstage.jst.go.jp/article/dmj/35/2/35_2015-255/_article.
48. Bilandžić MD, Wollgarten S, Stollenwerk J, Poprawe R, Esteves-Oliveira M, Fischer H. Glass-ceramic coating material for the CO_2 laser based sintering of thin films as caries and erosion protection. Dent Mater. 2017;33(9):995–1003.
49. Deliormanlı AM. Synthesis and characterization of cerium- and gallium-containing borate bioactive glass scaffolds for bone tissue engineering. J Mater Sci Mater Med. 2015;26(2):1–13.
50. Gao J, Li R, Wang F, Liu X, Zhang J, Hu L, et al. Determining the cytotoxicity of rare earth element nanoparticles in macrophages and the involvement of membrane damage. Environ Sci Technol. 2017;51(23):13938–48.
51. Pagano G, Aliberti F, Guida M, Oral R, Siciliano A, Trifuoggi M, et al. Rare earth elements in human and animal health: state of art and research priorities. Environ Res. 2015;142:215–20.

SUPPORTING INFORMATION

Additional supporting information may be found online in the Supporting Information section at the end of the article.

How to cite this article: Zambanini T, Borges R, Faria PC, et al. Dissolution, bioactivity behavior, and cytotoxicity of rare earth-containing bioactive glasses (RE = Gd, Yb). *Int J Appl Ceram Technol*. 2019;16:2028–2039. https://doi.org/10.1111/ijac.13317